Journal of Mechanical Engineering *Vol SI 5(2), 54-66, 2018*

Freestream Velocity Correction in Narrow Channels

Helmey Ramdhaney Mohd Saiah
Azmin Shakrine Mohd Rafie
*Fairuz I. Romli**
Department of Aerospace Engineering,
Faculty of Engineering, Universiti Putra Malaysia,
43400 Serdang, Selangor, Malaysia.

**fairuz_ir@upm.edu.my*

ABSTRACT

An experimental study was done on the effect of boundary layer development to freestream velocity in a narrow channel tunnel. Fundamental boundary layer theories were applied in quantifying and estimating the changes in the freestream velocity along the tunnel. It was found that the measured and the estimated freestream velocities were in good agreement. The increase in the freestream velocity was found due to the boundary layer blockage effect. The experimental results demonstrated that the corrected freestream velocity had negligible effect on the boundary layer analysis but it nevertheless proved to be a significant effect on correlating the flat plate heat transfer experiments.

Keywords: *heat transfer coefficient, boundary layer displacement thickness, blockage effect, velocity correction*

Introduction

Small experimental tunnels are typically used among researchers for simple experiments such as sensor calibrations, theoretical verification, testing new methodologies or theories, and many others before implementing them to the actual test rigs. Ease of access of these representative experimental tunnels made trial and error experiments more time and cost efficient. In designing an experimental tunnel, care must be taken to ensure that the development of the boundary layer will not affect the experiment as a whole. As the boundary layer develops along the wind tunnel, the tunnel will experience reduction in

ISSN 1823- 5514, eISSN 2550-164X
Received for review: 2017-04-28
Accepted for publication: 2017-06-05
Published: 2018-01-31

the cross sectional area. These reductions of area will continue until a fully developed flow is formed.

The fundamentals on this viscous affected phenomenon are found in Ref. [1]. Furthermore, Ref. [2] presented new parameters in determining the boundary layer velocity profile. Based on the results of several studies on flat plate with zero pressure gradient, the turbulent boundary layers will develop favourable pressure gradient along the flat plate [3, 4, 5]. This will cause the streamwise flow velocity to change in downstream direction of the flat plate. Development of turbulent boundary layer on a purely zero pressure gradient flow can be found in Ref. [6]. The boundary layer displacement thickness can be defined as the boundary layer blockage [7]. Ref. [8] states that boundary layers developed on the bounding walls will affect the internal flow. In heat transfer aspect, it is well known that increasing flow velocity would enhance heat transfer process. Hypothetically, on a zero pressure gradient flat plate, developing favourable pressure gradient by the boundary layers will cause an increase in the heat transfer process. In the study presented in Ref. [9], the researchers accelerated the freestream flow for a certain amount of time and length to investigate the effect of acceleration on the heat transfer process. They found an increase in Stanton number during the acceleration.

This research work is aimed to investigate the effect of boundary layer development in a narrow tunnel to its freestream velocity. It is expected that the freestream velocity of the wind tunnel will keep changing throughout the tunnel due to the boundary layer development. Mass flow continuity theory is used to get the corrected freestream velocity. The reason this issue is raised because in the flat plate heat transfer correlation, it involves the contribution of the Reynolds number in the equation. The freestream velocity used in the equation assumed that it is constant throughout the flat plate length. If this is the case in the experiment, no correction is required. But, if the freestream velocity did changed along the tunnel, then the freestream velocity needs to be corrected. The experiments are conducted to verify this issue.

Experimental Methods

A small experimental tunnel has been designed for the temperature sensor calibration and flat plate heat transfer experiment in the University of Bath, UK. The dimensions of the tunnel are 20 mm x 100 mm x 400 mm, as shown in Figure 1. These dimensions have been chosen to represent the wheel space dimensions in the single stage gas turbine representative test rig used by the Gas Turbine Research Group at the university. The internal structure of the test rig is made from stainless steel while the walls of the test rig are made from polycarbonate. Strips of neoprene foam are attached to the stainless steel internal structure to seal the test rig. The neoprene also acts as a thermal buffer due to its low thermal conductivity of 0.05 W/m^2K.

The bellmouth intake is designed according to the British Standard Long Radius Nozzle design [10]. Due to the rectangular design of the tunnel, modification to the design is made with the necessary diameter ratio required by the British Standard design is still maintained. The fabrication of the mesh heater is done by referencing the patent described in Ref. [11]. This heating element is fitted to ensure a step change of the air temperature during the heat transfer experiments. The transition section is designed based on Ref. [12]. A fast response thermocouple and an infrared sensor are used to measure the air temperature and the surface temperature history, respectively. The infrared sensor is fitted on the opposite side of the test surface in order not to disturb the test surface. Pressure measurements are acquired by using static and total pressure hypodermic tubes. In the boundary layer pressure measurements, the total pressure hypodermic tube is attached to a 0.5mm traversing mechanism.

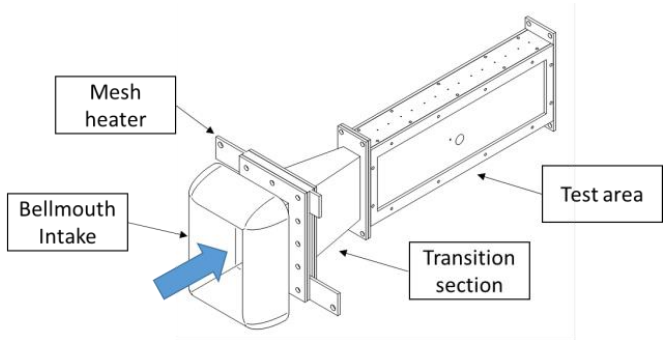

Figure 1: The experimental tunnel

Pressure Measurements

The turbulent boundary layer and the boundary layer displacement thickness can be easily obtained from the following Equation (1) and Equation (2), respectively [13].

$$\delta = 0.16x\,\mathrm{Re}_x^{-1/7} \tag{1}$$

$$\delta^* = \frac{1}{8}\delta \tag{2}$$

Moreover, the boundary layer blockage or blockage factor can be defined as shown in Equation (3), where W is the width of the channel [7].

$$BF = \frac{2\delta^*}{W} \tag{3}$$

The boundary layer blockage effect needs to be applied to all confining walls of the tunnel. The initial and effective areas of the tunnel are illustrated in Figure 2. Velocity at the core of the test area will increase with axial location due to the area reduction caused by boundary layer displacement thickness. The corrected velocity can be calculated using mass flow continuity equation as indicated by Equation (4).

$$\dot{m} = \rho U_1 A_1 = \rho U_2 A_2 \tag{4}$$

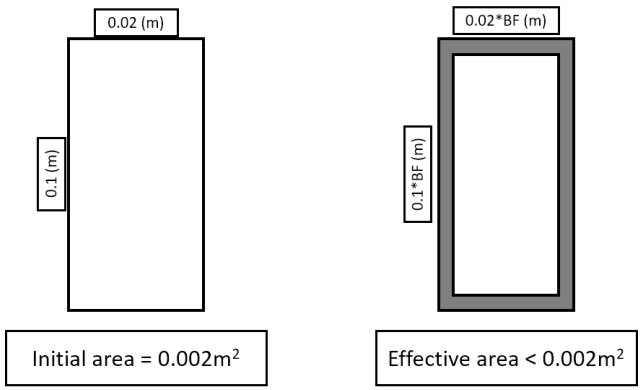

Figure 2: Changes in the test area

To verify the effects of boundary layer blockage in the experimental tunnel, pressure measurements are taken in the tunnel at three axial locations: immediate upstream (0.03m), mid-section (0.18m) and downstream region (0.33m), with all three location at the duct centerline. These locations are indicated in Figure 3.

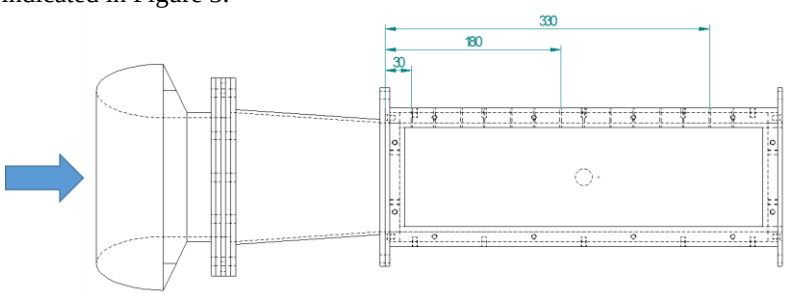

Figure 3: Pressure measurement for free stream velocity

The three measurements are converted to velocity values and they are represented by solid symbols in Figure 4 with values of 30.55 m/s, 33.18 m/s and 34.34 m/s. The velocity at location 0.03 m is taken into consideration in the calculation of corrected unchanged free stream velocity at initial location (0.00 m). It should be noted that any location can be chosen for the velocity correction procedure and the calculation will give a similar result. From the calculation, the corrected velocity at the initial condition is 30.02 m/s. The accelerated velocities due to the boundary layer blockage along the tunnel are estimated and represented by the dotted line in Figure 4. This result further confirms that boundary layer blockage can be used to estimate the accelerated flow in a small tunnel.

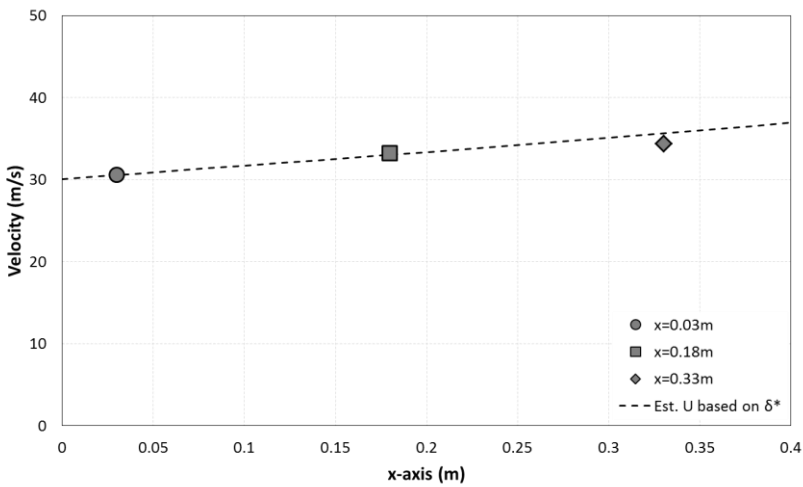

Figure 4: Estimation of flow acceleration

Boundary Layer Thickness

The pressure measurements are made by traversing the y-axis at x = 0.18 m to acquire the boundary layer thickness. The measurements are shown in Figure 5, which are represented by the open circle symbols. The freestream velocity is measured as 39.91 m/s and at 99% of this value, the boundary layer thickness is found to be 4.79 mm. By applying the blockage factor, the corrected velocity is 34.51 m/s. Using the boundary layer thickness equation, the calculated theoretical boundary layer thickness is 4.66 mm. It should be noted that the difference between the experimental and theoretical results is only 2.8%. From this finding, it can be said that the effect of boundary layer blockage can be considered negligible if it only involves the boundary layer

analysis. However, the same could not be said for the flat plate heat transfer analysis.

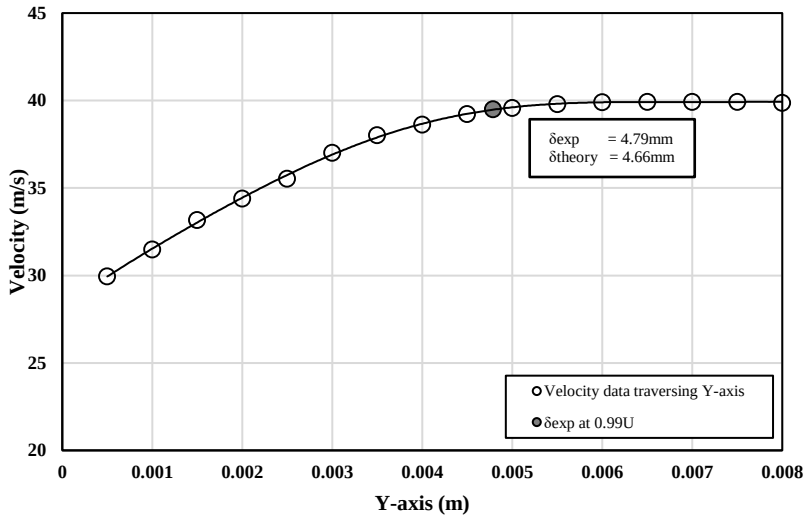

Figure 5: Boundary layer measurement

Flat Plate Heat Transfer

In the flat plate heat transfer experiments, a fast response mesh heater is used to induce a step change in air temperature. For temperature measurements, a fast response thermocouple is used to acquire the air temperature history and an infrared sensor is used to capture the local surface temperature history. The infrared sensor is placed at x = 0.2 m and the fast response thermocouple is placed at the immediate downstream from the infrared sensor. The pressure measurement is taken at x = 0.33 m. Thermocouples and pitot-static tubes are categorized as intrusive instruments, therefore it is recommended that these type of instruments are located at downstream region to avoid obstruction to the flow structure that might subsequently disrupt the thermal behaviour at surface temperature measurement location. As previously discussed, pressure measurements can be made at any location and corrected free stream velocity can be properly estimated. The measured freestream velocity is 39.18 m/s and the corrected freestream velocity is 33.87 m/s.

Figure 6 presents the air and surface temperature history. The dotted gray line represents the surface temperature history for an insulation type material, polycarbonate that possess thermal conductivity characteristic of 0.2

W/mK.The surface temperature history is measured by the Melexis infrared sensor located on opposite plate of the test surface plate. The infrared sensor has been calibrated in the tunnel with uncertainty of ± 0.2 °C. In Figure 6, the solid black line represents the air temperature history measured by a type-K fast response thermocouple. This fast response thermocouple is calibrated in a constant temperature bath with limits of error of ± 0.1 °C. At a corrected freestream velocity of 33.87 m/s, the average measure of the working air temperature is 38.6°C with RMS error of 0.2 °C. The measured initial surface temperature, T_{si} is found to be 22.2°C.

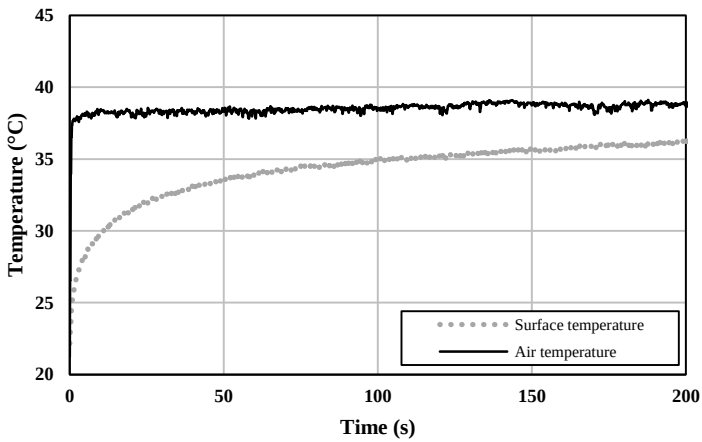

Figure 6: Air and surface temperature history data

The surface temperature history data is analysed using Crank Nicolson heat equation model with a forced convection-conduction condition at the test surface and an adiabatic condition for the back surface of the test plate. In order to ensure an adiabatic condition and no heat transfer process occurs at the back surface, an experimental time limit is imposed to the heat transfer experiments. The time limit is obtained by Equation (5), which is based on Ref. [14] and assuming a semi-infinite solid condition. α in Equation (5) is the thermal diffusivity of the test plate material.

$$t_L = \frac{L^2}{9\alpha} \tag{5}$$

With the boundary conditions set, the Crank Nicolson heat equation can be rewritten as Equation (6), Equation (7) and Equation (8) as follow:

- Target surface with forced convection-conduction condition

$$-2BiFo(T_\infty)+2(BiFo+1+Fo)(T_i^{n+1})-2Fo(T_{i+1}^{n+1}) = 2BiFo(T_\infty)+2(-BiFo+1+Fo)(T_i^n)+2Fo(T_{i+1}^n) \quad (6)$$

- Internal nodes with one dimensional heat conduction

$$-Fo(T_{i-1}^{n+1})+2(1+Fo)(T_i^{n+1})-Fo(T_{i+1}^{n+1}) = Fo(T_{i-1}^n)+2(1+Fo)(T_i^n)+Fo(T_{i+1}^n) \quad (7)$$

- Back surface with adiabatic condition

$$-2Fo(T_{i-1}^{n+1})+2(1+Fo)(T_i^{n+1}) = 2Fo(T_{i-1}^n)+2(1-Fo)(T_i^n) \quad (8)$$

where $Bi=\frac{h\Delta x}{k}$ and $Fo=\frac{\alpha t}{L^2}$

With reference to Equation (5), the surface temperature history data could only be used up to t = 168 seconds for the test plate to remain in semi-infinite solid condition. The maximum surface temperature, T_s at this t = 168 seconds is 35.9 °C. The resultant surface heat flux is presented in Figure 7. Relationship between the surface heat flux and the convective heat transfer coefficient can be represented by Equation (9) [15].

$$q = h(T_{aw} - T_s) \quad (9)$$

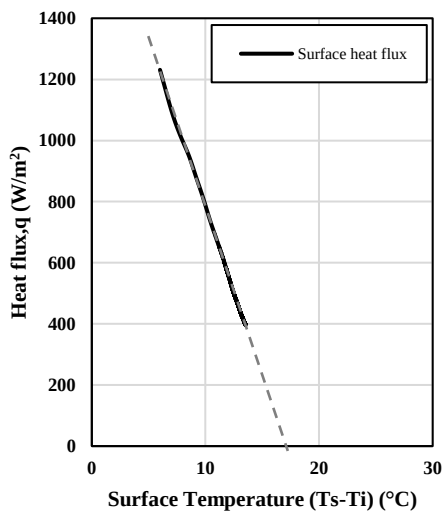

Figure 7: Surface heat flux

The slope of graph in Figure 7, obtained through linear regression, is the convective heat transfer coefficient, h. At q = 0, the surface temperature, T_s is the same as the adiabatic wall temperature, T_{aw}. In this particular case, the heat transfer coefficient and adiabatic wall temperature are h_x= 110.93 W/m^2 and T_{aw}= 39.2 °C, respectively. To verify the heat transfer coefficient, the experimental heat transfer coefficient is compared to the flat plate heat transfer coefficient, h_{FPx} as given by Equation (10) [16].

$$h_{FPx} = 0.0296 \rho c_p U_\infty \mathrm{Pr}^{1/3} \mathrm{Re}_x^{4/5} \tag{10}$$

At the uncorrected freestream velocity, U_{UC} = 39.18m/s, h_{FPx} equals to 120.11 W/m^{2}K. Meanwhile, when corrected freestream velocity, U_C = 33.87 m/s, h_{FPx} is equals to 106.9 W/m^{2}K. For this particular case, it is found that if the user chose uncorrected freestream value, error between the experimental result and the correlation is 7.6%. A much smaller error of 3.7% is achievable if the user chose the corrected freestream value. Figure 8 shows the result of the flat plate experiments for boundary layer analysis and the heat transfer coefficient over a range of Reynolds numbers.

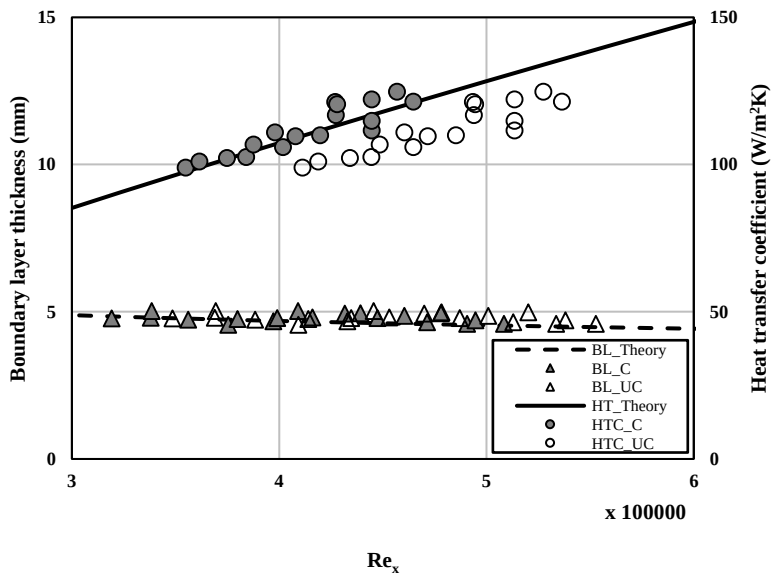

Figure 8: Flat plate boundary layer and heat transfer coefficient

In Figure 8, the open symbols represent the experimental data with the uncorrected freestream velocity whereas the solid symbols represent the experimental data after having the freestream velocity corrected for each

case. Moreover, the triangular symbols represent boundary layer analysis data and the round symbols represent heat transfer coefficient. Theoretical correlations are represented in lines. Boundary layer theoretical values are presented by dashed line while flat plate heat transfer correlation values are presented by solid black line. The boundary layer data is plotted on the primary y-axis on left hand side of the graph. The heat transfer coefficient data is plotted on the secondary y-axis on right hand side of the graph. All the experimental data is plotted against the Reynolds numbers.

It seems that insignificant effect can be found on the boundary layer analysis, which agrees well with previously shown data on a single boundary layer analysis case. This is not the case with the heat transfer experiments. It can be observed that significant changes are evident in the shifting of the whole heat transfer coefficient experimental data when freestream velocities are corrected. Note that the experimental heat transfer coefficient data does not change, only the corresponding Reynolds numbers are changed. The main reason for this shift in the experimental data is because of the heat transfer correlation used. The correlation used is made for flat plate heat transfer condition where the freestream velocity remains constant along the flat plate. It can also be used in a wide tunnel where effects of the favourable pressure gradient due to the boundary layer does not affect the freestream velocity and the cross sectional area is uniform. However, this is not the case for current experimental setup where the freestream velocity in the narrow channel is affected by the developing boundary layer.

Conclusion

The purpose for the experimental rig is to perform fundamental heat transfer studies in order to investigate techniques that will improve the accuracy and reliability in the measurement of heat transfer coefficient and corresponding adiabatic wall temperature. The tunnel is designed to represent the wheel space area for turbine disc cooling in single stage gas turbine representative rig in which the flow conditions are more complex. Due to the rectangular shape where the hydraulic diameter could not be correctly approximated, it is highly inappropriate to correlate the heat transfer process in the tunnel with the Dittus-Boelter correlation for heat transfer in a tube. The Dittus-Boelter correlation is primarily meant for fully developed turbulent flow in smooth tubes, which is not the case for the current research work.

The results have shown that, without considering the boundary layer blockage effect in narrow experimental channels, users will not be able to properly correlate and also justify the experimental flat plate heat transfer coefficient data. The comparison between experimental data and theoretical data highlights that the former data is being underestimated in such condition. More damages are to be expected if the user neglects this issue and tend to

make a new correlation just because the narrow rectangular channels could not be correlated with either the flat plate heat transfer correlation or any other correlation involving flow in a closed conduit.

Nomenclature

A	area
Bi	Biot number
BF	blockage factor
BL	boundary layer
c	specific heat
Fo	Fourier number
h	heat transfer coefficient
HT	heat transfer
k	thermal conductivity
$\dot{m}$	mass flow rate
Pr	Prandtl number
q	heat flux
Re	Reynolds number
RMS	root mean square
T	temperature
t	time
U	velocity
W	channel width

Greek Symbols

α	thermal diffusivity
δ	boundary layer thickness
δ^*	boundary layer displacement thickness
ρ	density

Subscript

aw	adiabatic wall
C	corrected
exp	experimental
FP	flat plate
i	location step
L	thickness of plate
p	pressure
s	surface data
si	initial surface data
theory	theoretical
UC	uncorrected
x	axial location

Superscript

n time step

Acknowledgement

The authors acknowledge the funding for this research by the Ministry of Education, Malaysia and Universiti Putra Malaysia. In addition, the authors would like to thank Dr. Kevin Robinson, Prof. Gary Lock and Prof. Michael Owen from University of Bath for their guidance in this study.

References

[1] H. T. Schlichting, Boundary layer theory (The McGraw-Hill Companies, New York, 1968)
[2] D. W. Weyburne, "New thickness and shape parameters for the boundary layer velocity profile," Experimental Thermal and Fluid Science 54, 22-28 (2014).
[3] S. J. Kline, W. C. Reynolds, F. A. Schraub and P. W. Runstadler, "The structure of turbulent boundary layers," Journal of Fluid Mechanics 30 (4), 741-773 (1967).
[4] D. B. DeGraaff and J. K. Eaton, "Reynolds-number scaling of the flat-plate turbulent boundary layer," Journal of Fluid Mechanics 422, 319–346 (2000).
[5] G. F. Oweis, E. S. Winkel, J. M. Cutbrith, S. L. Ceccio, M. Perlin and D. R. Dowling, "The mean velocity profile of a smooth-flat-plate turbulent boundary layer at high Reynolds number," Journal of Fluid Mechanics 665, 357-381 (2010).
[6] I. Marusic, K. A. Chauhan, V. Kulandaivelu and N. Hutchins, "Evolution of zero-pressure-gradient boundary layers from different tripping conditions," Journal of Fluid Mechanics 783, 379-411 (2015).
[7] E. M. Greitzer, C. S. Tan and M. B. Graf, Internal Flow - Concepts and Applications (Cambridge University Press, Cambridge, 2004).
[8] D. T. Squire, C. Morrill-Winter, N. Hutchins, M. P. Schultz, J. C. Klewicki and I. Marusic, "Comparison of turbulent boundary layers over smooth and rough surfaces up to high Reynolds numbers," Journal of Fluid Mechanics 795, 210-240 (2016).
[9] W. M. Chakroun and R. P. Taylor, "Experimental investigation of the effects of acceleration on heat transfer in the turbulent boundary layer," 13th Workshop for Computational Fluid Dynamic Application in Rocket Propulsion and Launch Vehicle (1996).

[10] BSi, Measurement of fluid flow by means of pressure differential devices inserted in circular cross-section conduits running full. Part 3: Nozzles and venturi nozzles (2003).
[11] P. T. Ireland, D. R. Gillespie and Z. Wang, US Patent No. US6181874 B1 (30 January 2001).
[12] P. P. Walsh and P. Fletcher, Gas turbine performance (Blackwell Science Ltd., Oxford, 2004).
[13] F. M. White, Fluid Mechanics (McGraw-Hill Education, New York, 2010).
[14] D. L. Shultz and T. V.,"Heat Transfer measurement in short duration hypersonic facilities," Advisory Group for Aerospace Research and Development, Paris, France (1973).
[15] D. O'Dowd, Q. Zhang, L. He, P. Ligrani and S. Friedrichs, "Comparison of heat transfer measurement techniques on a transonic turbine blade tip," Journal of Turbomachinery 133, (2011).
[16] J. P. Holman, Heat Transfer (McGraw-Hill Education, New York, 2009).